Colloid Polym Sci 279:1073–1081 (2001)

ORIGINAL CONTRIBUTION

J. Chatterjee
Y. Haik
C.-J. Chen

Synthesis and characterization of heat-stabilized albumin magnetic microspheres

Received: 12 September 2000
Accepted: 5 February 2001

J. Chatterjee · Y. Haik (✉) · C.-J. Chen
Department of Mechanical Engineering
Biomagnetic Engineering Laboratory
FAMU-FSU College of Engineering
2525 Pottsdamer Street, Tallahassee
FL 32310, USA
e-mail: haik@eng.fsu.edu
Tel.: +1-850-4106431
Fax: +1-850-4106480

Abstract Human serum albumin magnetic microspheres containing 30% iron oxide particles were synthesized by a heat-stabilization process. The average diameter, the size distribution and the morphology were characterized by scanning electron microscopy, atomic force microscopy and transmission electron microscopy. The distribution of the iron oxide nanoparticles within the microspheres was confirmed by the contrast obtained in the morphology by backscattered electron imaging in scanning electron microscopy. Energy-dispersive X-ray spectroscopy showed the presence of iron in the microspheres. The cabbage like surface structure in some of the microspheres obtained in scanning electron microscopy can be better understood by atomic force microscopy. This peculiar surface structure in the microsphere may be due to the cross-linking in the protein molecule by heat. The amount of iron oxide in the microsphere was analyzed by atomic absorption spectroscopy. The magnetic properties of the particles were measured in a superconducting quantum interference device magnetometer.

Key words Human serum albumin · Magnetic microsphere · Heat stabilization · Atomic force microscopy · Backscattered electron

Introduction

Albumin encapsulated magnetic microspheres have been reported to have potential in several biomedical applications, such as cell separation [1–4], diagnosis [5, 6] and targeted drug delivery [7–12]. Earlier, we reported the synthesis and use of chemically cross-linked albumin magnetic microspheres for the separation of red blood cells from whole blood [13]. In that case chemical cross-linking was done using glutaraldehyde and the chemically cross-linked microspheres were modified with lectin, a carbohydrate binding protein that effectively couples with red blood cells. The chemically cross-linked microspheres showed nonuniform sizes and aggregates. This behavior was also reported by Gupta and coworkers [14, 15]. In this article we report the synthesis of albumin magnetic microspheres in the submicron and micron range using nanosized magnetic particles. The microspheres were stabilized by thermal treatment of the protein human serum albumin (HSA). The heat treatment causes the formation of intermolecular disulfide bridges between the free SH groups on adjoining protein chains. Thus, the thermal denaturation is a curing process that yields a chemically cross-linked polymer network structure. These heat-stabilized albumin magnetic microspheres are found to be more stable and are more polydisperse than those of the chemically cross-linked microspheres.

The size characterization of these microspheres is important for magnetic blood cell separation, cell sorting, diagnosis and drug delivery [16]. The size distribution and the magnetic properties of the microspheres are important for different applications. The magnetic force that is needed to isolate the magnetic

microsphere from the fluid is proportional to the volume of the magnetic material entrapped in the microspheres, its magnetic properties, the magnetic field strength and the magnetic field gradient. Scanning electron microscopy (SEM) is the most common and widely used tool for characterizing the microspheres in terms of size, shape and the surface characteristics. The structures of the macromolecules, for example, proteins and nucleic acids, have been observed by atomic force microscopy (AFM) recently [17–19] and AFM can be used to obtain the surface characteristics of the microspheres in detail. Both SEM and AFM were used to characterize the albumin microspheres.

The amount of magnetic material encapsulated in the microsphere and its location are important factors when considering the characteristics of any magnetic microsphere. Any microsphere, even with adsorbed magnetic particles, may behave as a magnetic microsphere and will respond to an external magnetic field; however, this class of material would not be considered as a stable magnetic microsphere as the adsorbed magnetic particle may detach from the surface during washing or a change of temperature or pH of the medium. In order to classify the microspheres as stable magnetic microspheres the location of the magnetic particle should be inside the microsphere. The use of confocal microscopy to show the contrast due to the presence of a magnetic particle within the sphere has been reported [20]. Transmission electron microscopy (TEM) can be a very important characterization technique to show the distribution of particles inside the microsphere, especially when they are in the submicron range. The capability of using backscattered electron microscopy to produce compositional contrast has existed since the 1960s. In present study the backscattered electron imaging mode of SEM was used to show the contrast due to the presence of an iron oxide particle in the sphere. This image obtained by backscattered electrons is different from the secondary electron image in terms of the inner morphology of the microsphere.

The signal for the iron present in the microspheres was detected by energy-dispersive X-ray analysis (EDXA). A JSM 5900 was used for EDXA in different places of a microsphere. The results showed that the magnetic particles were more or less evenly distributed in the microsphere but did not cover the entire volume of the sphere.

TEM was performed on γ-Fe_2O_3 (maghemite) particles to show their size distribution. TEM of the albumin microspheres was also performed to show the presence of magnetic iron oxide particles inside the microsphere.

The magnetic force on microspheres that encapsulate superparamagnetic material is proportional to the volume of the magnetic material and the magnetic properties of the material. A high maghemite content in the sphere will need a lower magnetic field to affect the motion. The iron content in the microspheres was measured by atomic absorption spectroscopy. The magnetic properties of the microspheres were measured using a superconducting quantum interference device (SQUID) magnetometer. The measurements showed that the magnetic microspheres synthesized have superparamagnetic characteristics.

Experimental

HSA, cottonseed oil, was obtained from Sigma Chemical Company. Iron oxide (maghemite, γ form of Fe_2O_3 with an average particle size of 26 nm) was obtained from Nanotechnolgy Corporation.

Synthesis of the albumin magnetic microsphere

HSA (250 mg) was dissolved in a dispersion of 75 mg iron oxide (~30% of the weight of HSA) in 1 ml distilled water and was

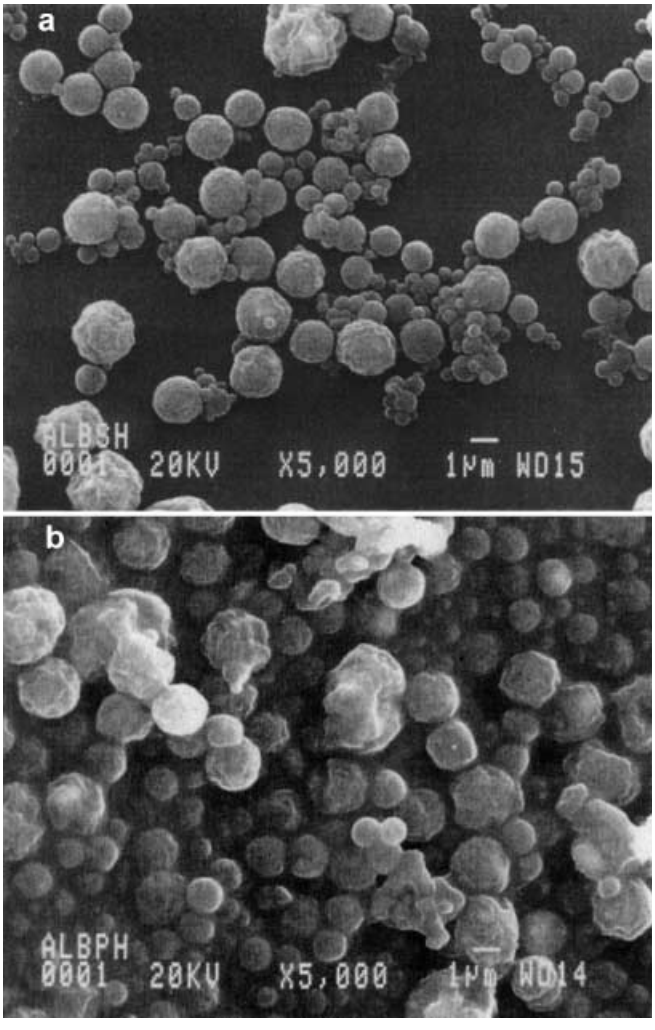

Fig. 1 Scanning electron microscopy (*SEM*) of an albumin magnetic microsphere sample **a** from dispersion and **b** in powder form

finally added to 30 ml cottonseed oil containing 0.2 ml sorbitan sesquioleate. The mixture was then shaken vigorously and then sonicated (Cole Parmer ultrasonic homogenizer) for three 30-s intervals at an amplitude of 60%. The sonication process was done at 4 °C using an ice–water bath. This primary emulsion was then added dropwise to 100 ml cottonseed oil heated at 130 °C and stirred at 1500 rpm. The whole addition was done in 10 min. The mixture was kept at 130 °C with the same stirring speed (1500 rpm) for another 15 min. The heat-stabilized microspheres were then cooled and extracted with diethyl ether. The microspheres were washed by adding diethyl ether to the microspheres and centrifuging. After washing three times with diethyl ether, the dispersion of the microspheres in ether was filtered successively using nylon filter membranes (Pall Speciality Chemicals) with pore sizes of 3, 1.2, 0.8, 0.65, 0.45 and 0.30 μm. The microspheres were retained on the filter papers except for the one with 3 μm pore size. A total of 300 mg microspheres was obtained from all the filter membranes and of that approximately 250 mg was collected from the filter membranes with pore sizes of 1.2, 0.8 and 0.65 μm. The microspheres were then dried in air and stored in a vacuum desiccator.

Scanning electron microscopy

SEM was performed using a JSM 840 (Jeol) and a JSM 5900 microscope. The samples were placed on carbon tape when they were in powder form and on glass cover slips when they were taken from suspension and mounted on aluminium stub. The samples were coated with gold–palladium (about 15-nm thickness) and were observed under 20 keV for both secondary and backscattered

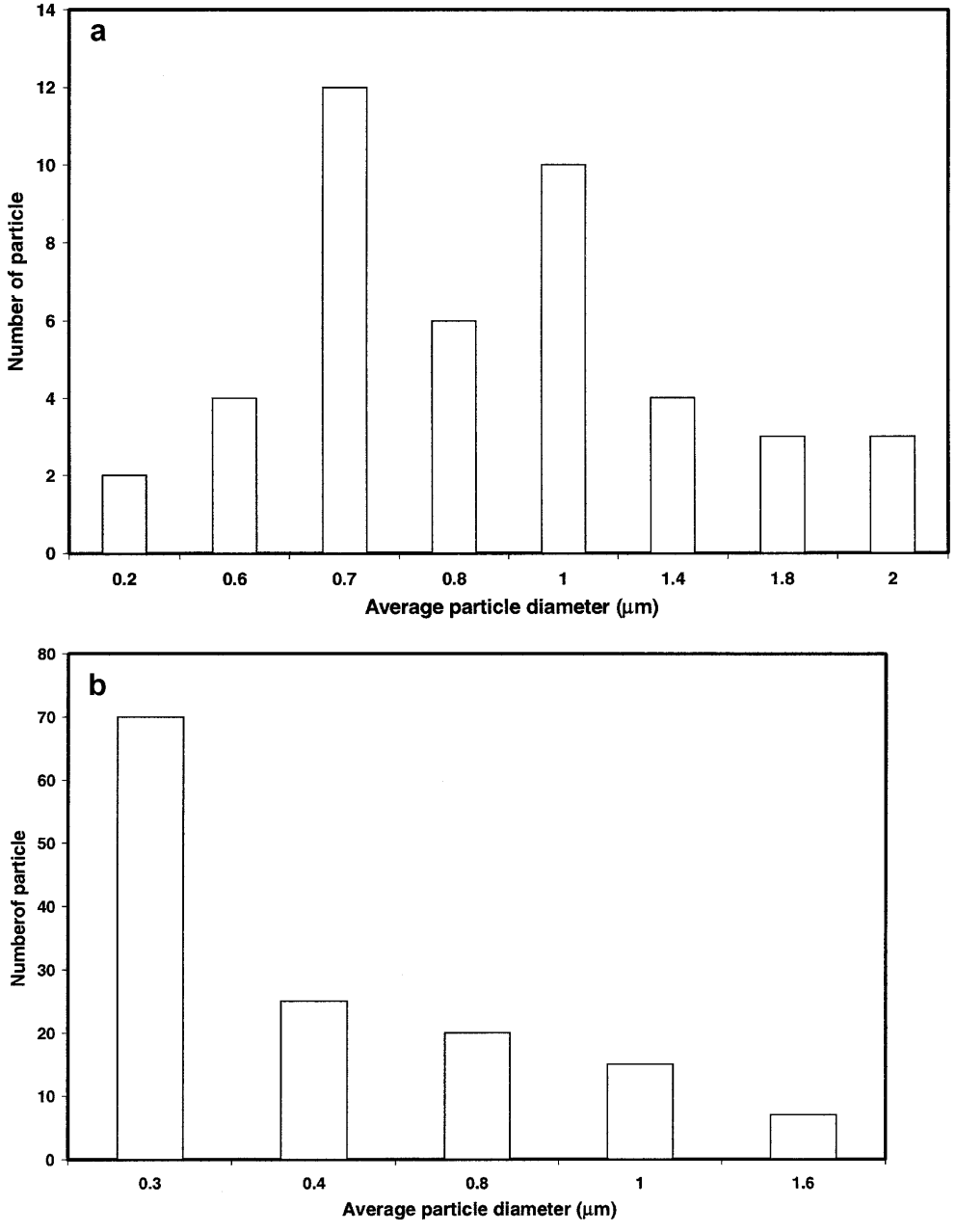

Fig. 2 Histogram for the particle size distribution as obtained from SEM **a** in dispersion and **b** in powder form

electron imaging. The incident beam energy was chosen as 20 keV. The backscattering coefficient increases slightly with the incident beam energy (between 10 and 30 keV) for the elements with atomic number less than 47 [21].

EDXA samples were taken in carbon tape and mounted on a carbon stub in order to avoid signals for aluminum (from the aluminum stub) and silicon (from the glass cover slip).

Atomic force microscopy

A D-3000 (Digital Instruments, Santa Barbara) atomic force microscope was used in this study. Samples were deposited on glass slides coated with poly(L-lysine) solution and then washed with distilled water and dried. Poly(L-lysine) creates a charged surface that helps to immobilize the albumin magnetic microspheres nicely on the glass surface. Magnetic force microscopy (MFM) was performed with the same sample as for AFM, except the tip was magnetic in MFM.

Atomic absorption spectrometry

A PerkinElmer Zeeman 5100 furnace atomic absorption spectrophotometer was used to determine the iron concentration in the microspheres. The analysis utilized pyrolytically coated graphite tubes equipped with L'vov platforms. Samples (of the order of a few micrograms) were suspended in 10 ml 0.2% nitric acid and digested using a CEM microwave (model MDS 2000). After digestion, the samples were made up to 1,000 ml with MilliQ water and were analyzed in the spectrophotometer.

Transmission electron microscopy

A JSM 2010 scanning transmission electron microscope was used to determine the size of the maghemite particles and to show the presence of maghemite inside the albumin microspheres. A drop of very dilute solution of both the maghemite and the albumin microspheres was placed on a carbon-coated copper grid and the diameter was determined from the micrograph.

Measurement of magnetic properties

A Quantum Design MPMS5 DC SQUID magnetometer was used to study the magnetic properties of the maghemite particles and the albumin magnetic microspheres. Samples were placed in a gelatin chamber and then inserted into the SQUID chamber. The magnetization measurements were done under both zero-field cooled (ZFC) and field cooled (FC) conditions with an applied constant field of 50 G. The magnetization at different applied magnetic fields ranging from –5 to 5 T was also measured at both 5 and 300 K.

Results and discussion

Scanning electron micrographs of the heat-stabilized microspheres obtained from dispersion and from powder are shown in Fig. 1a and b. The size distributions are observed in the histogram in Fig. 2a and b. The average particle sizes were 0.8 and 1 μm, respectively. It is evident from the micrograph that these microspheres are not agglomerated. The cabbage-like surface structure is probably due to the cross-linking of albumin protein by heating. In fact heating allows the evaporation of water from the emulsified droplet of protein and thus ensures the rigidity of the sphere [22]. SEM micrographs for

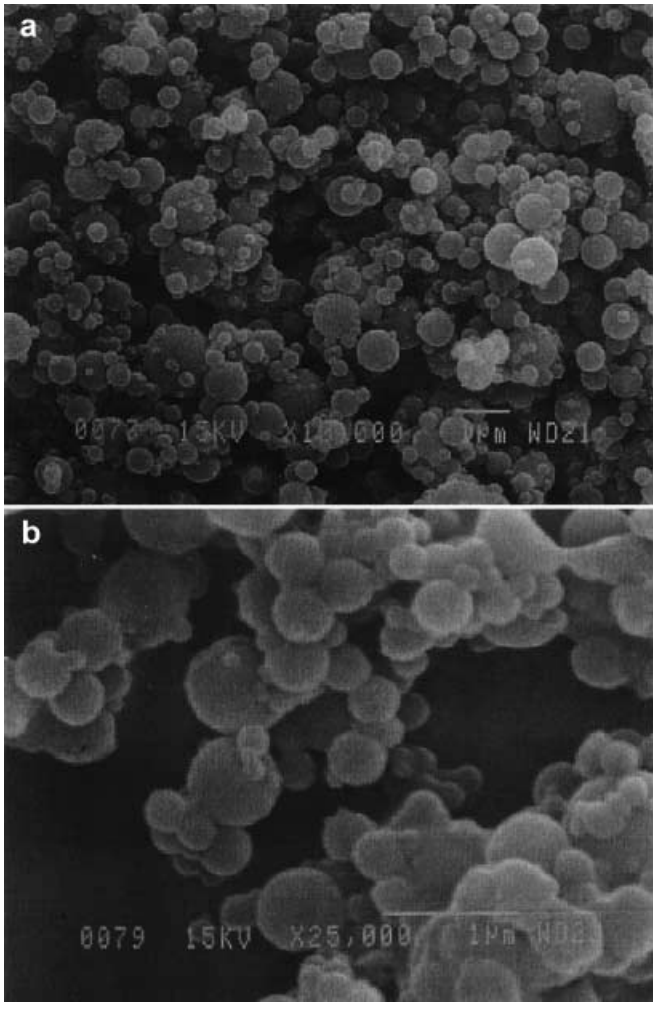

Fig. 3a, b SEM of chemically stabilized albumin microsphere

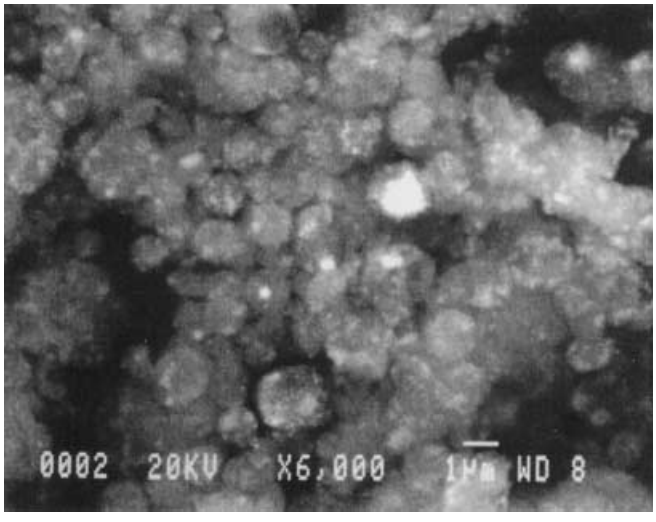

Fig. 4 SEM of albumin microspheres in powder form, backscattered electron image

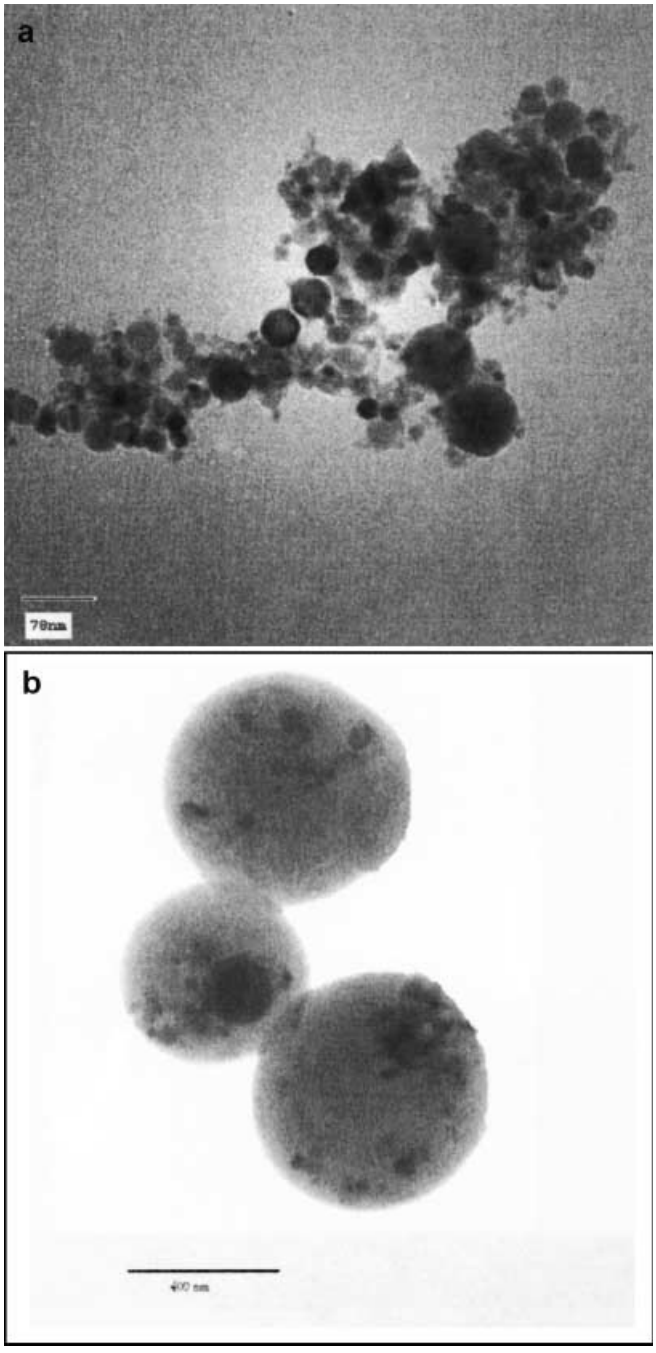

Fig. 5 Transmission electron microscopy (*TEM*) micrographa of **a**maghemite (γ Fe_2O_3) powder and **b** albumin magnetic microspheres

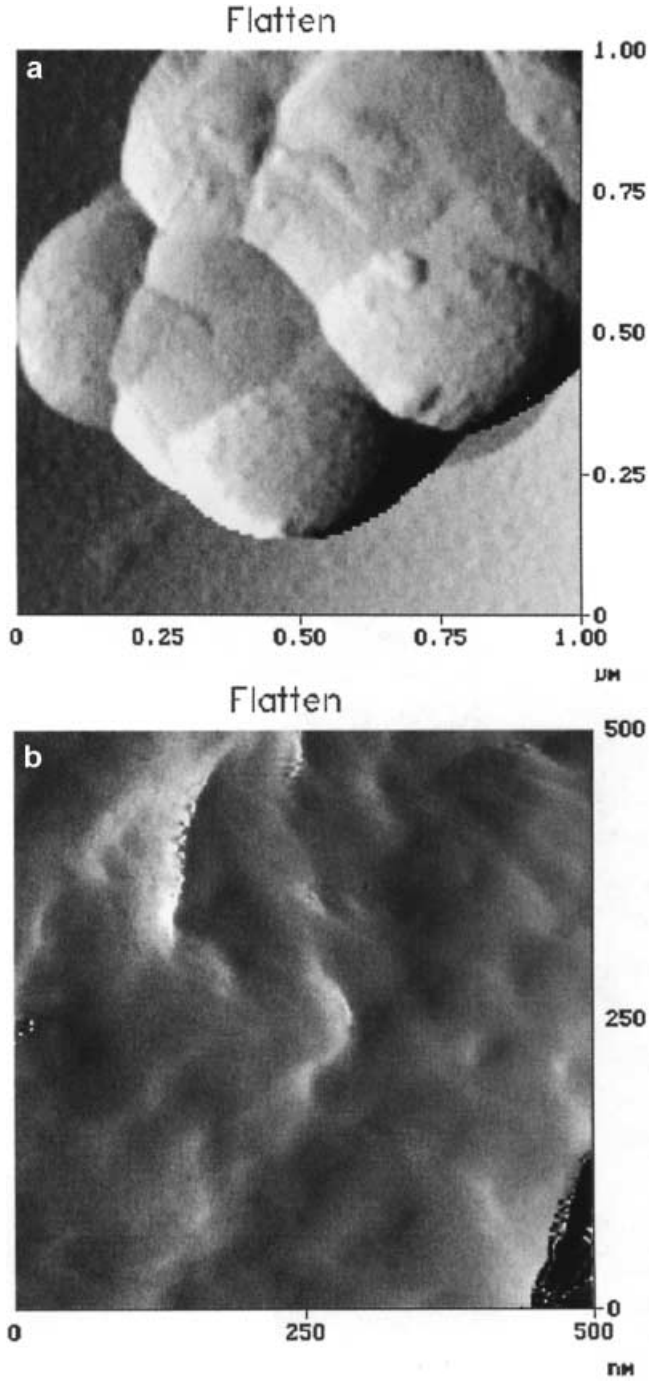

Fig. 6 **a** Surface structure in phase mode and **b** flattened view of the surface structure in height mode on an enhanced scale

chemically stabilized particles are shown in Fig. 3a and b. Here the surface remains smooth. The method of synthesis for chemically stabilized microspheres is described elsewhere [13]. These microspheres have a wide size distribution, though most of them are in the submicron range; however, irrespective of the sizes, their surface does not show any special morphology, unlike the heat-stabilized microspheres.

Figures 1 and 3 are the secondary electron images conventionally used for observation of morphology. The backscattered electron image for the same sample of the heat-stabilized microsphere is shown in Fig. 4. Secondary electrons have low energy and are unlikely to escape from the specimen if produced at a depth of 50

below the surface; thus, they provide the finer detail of the surface. Backscattered electrons have more energy than 50 eV, the backscattering coefficien, η, is usually defined as the ratio of the number of backscattered electrons to the number of incident electrons [21]. η varies markedly with the atomic number [23, 24]. The contrast in the internal morphology of the particles shown in Fig. 4 is due to the incorporated iron oxide. The contrast is observed from both discrete nanosized particles and from agglomerated particles. TEM micrographs of the iron oxide particles and the albumin microspheres are shown in Fig. 5a and b, respectively. Figure 5a shows the wide range of particle sizes in the maghemite used.

AFM gives the finer detail in the cabbagelike structure of the microsphere. The surface structure of the microsphere in phase mode is shown in Fig. 6a. The surface structure of the same sphere in height mode on an enhanced scale is shown in Fig. 6b. The cracks and crevices observed in this structure are due to heat cross-linking as confirmed by the surface morphology of both the heat-stabilized and the chemically stabilized microspheres as shown in Figs. 1 and 3, respectively. MFM was also performed; however, no contrast was obtained owing to the presence of the magnetic particle in the microsphere. This could be due to the fluctuation of the magnetization of the particles owing to the applied field at the tip of the scope and the quasispherical magnetic particles.

The EDX of the microspheres as obtained using a JSM 840 is shown in Fig. 7. The signal for the iron (from the magnetic particle) was obtained clearly at 6.403 keV for Fe Kα and at 7.057 keV for Fe Kβ. For the sulfur (present in the albumin molecule) the signal was obtained at 2.3 keV.

Atomic absorption analysis shows approximately 32% iron in the microspheres. This amount is much higher than the chemically cross-linked microsphere (about 20%) reported earlier [13].

Temperature–susceptibility plot at 50 G for the ZFC and FC cases for γFe_2O_3 and both heat-stabilized and chemically stabilized albumin magnetic microspheres are shown in Fig. 8a and b, respectively. In the ZFC case the sample is brought to 5 K while the applied field is maintained at zero. When the temperature stabilizes at 5 K an applied field of 50 G is imposed on the sample. The temperature is then raised in steps of 10 K. The SQUID that is used in this experiment is limited to 300 K. Once the temperature reaches 300 K the sample is cooled back to 5 K in steps of 10 K while the applied field remains at 50 G (FC). Initially an increase in the susceptibility with temperature was observed in the ZFC data, as there was no applied field; the particles all had a random orientation of their magnetizations. When a small field is applied and thermal energy is added to the sample, the smaller particles will have an amount of energy comparable to their energy barrier. Thus, their magnetization aligns in the direction of the applied field

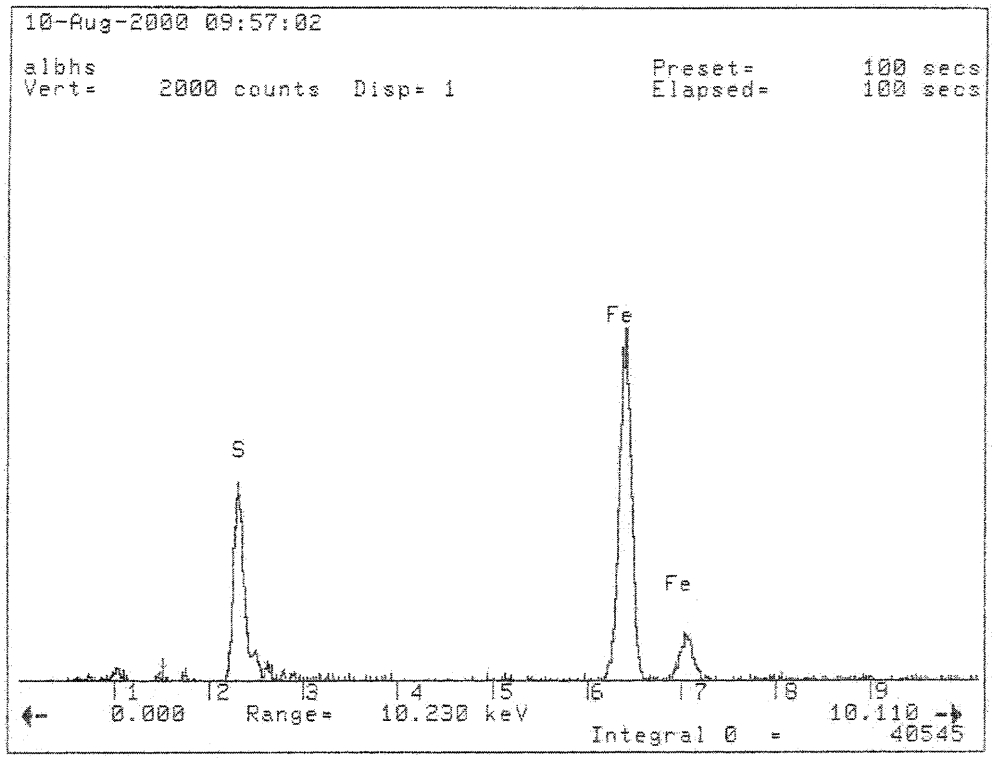

Fig. 7 Energy-dispersive X-ray analysis of albumin microspheres

and an increase in the sample magnetization is observed with temperature. Because of the significant distribution of particle sizes from submicron to more than 1 μm, there will be a range of blocking temperatures depending on the particle sizes. Thus, we did not observe a blocking temperature (temperature below which the particle moments are blocked and it is usually determined by measuring the peak position of the ZFC susceptibility versus temperature curve [25] even at room temperature. As the sample was cooled in a constant applied magnetic field, the thermal energy was being reduced, which allowed the particles to fix their magnetic moment in the

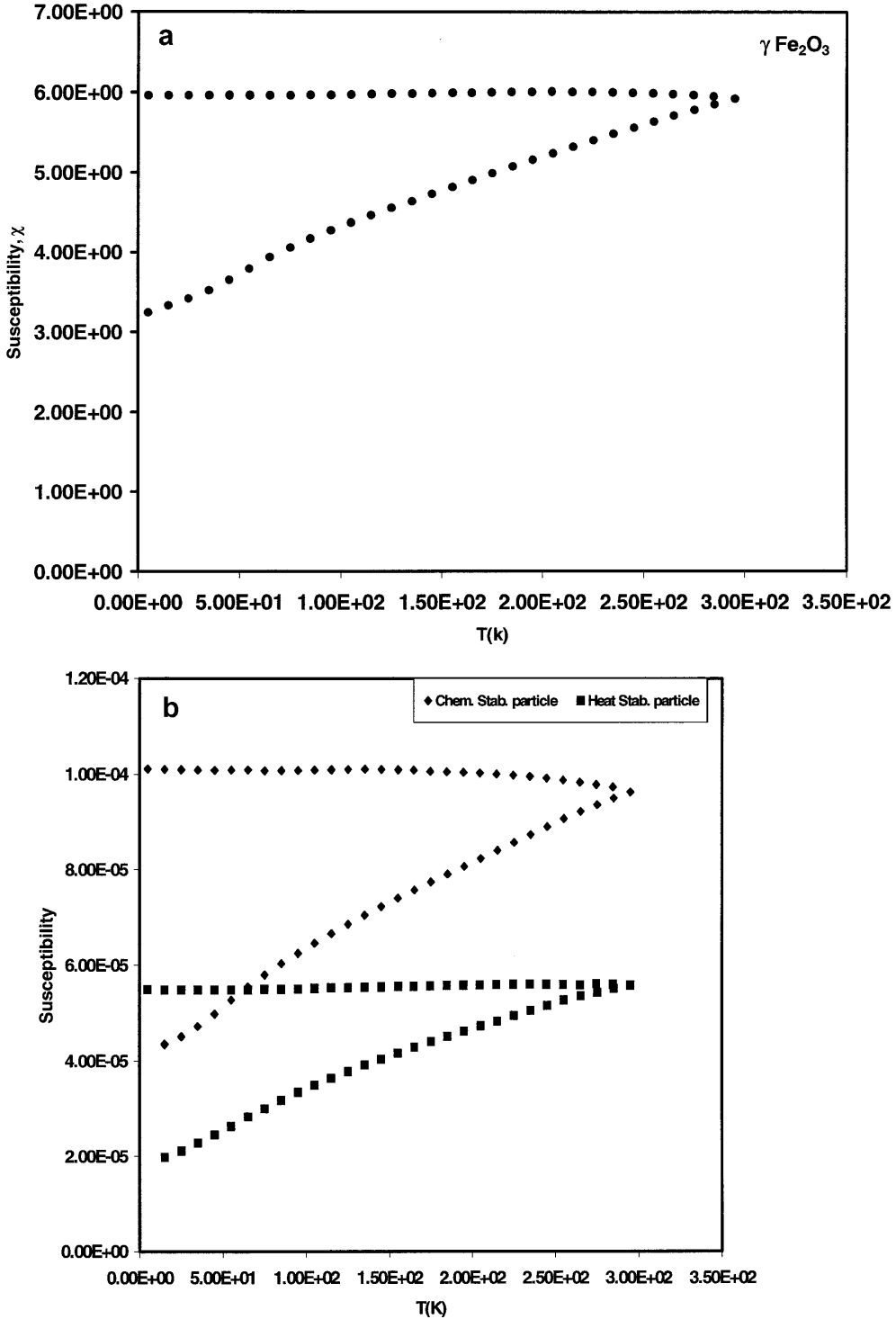

Fig. 8 **a** Temperature–susceptibility plot for γ Fe_2O_3. **b** Temperature–susceptibility plot for both chemically stabilized and heat-stabilized albumin magnetic microspheres

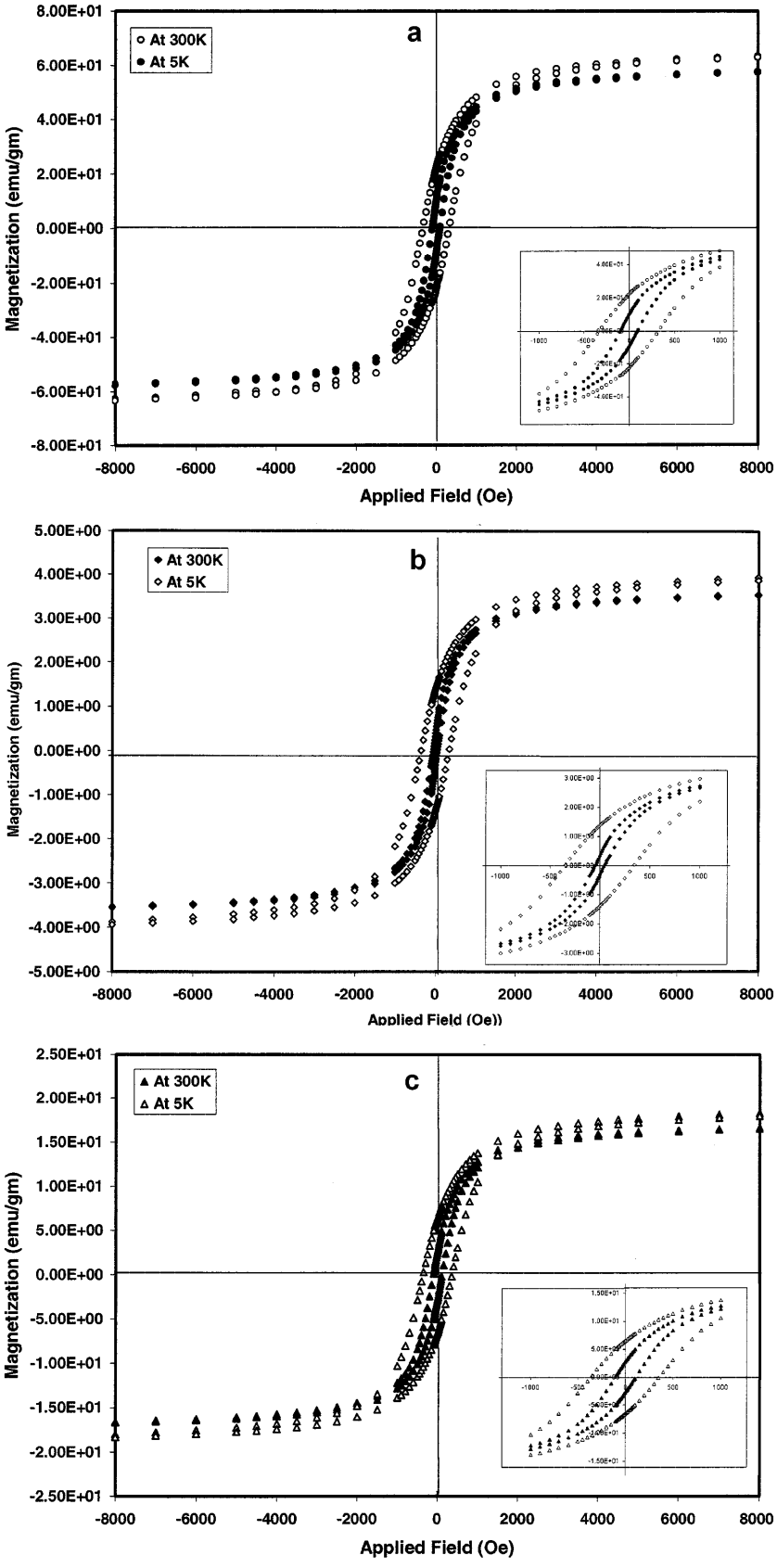

Fig. 9 Applied field versus magnetization plot **a** for γ Fe_2O_3, **b** for chemically stabilized albumin magnetic microspheres and **c** for heat-stabilized albumin magnetic microspheres

direction of the magnetic field. Thus almost no change in the susceptibility was observed.

The magnetization at 5 and 300 K is shown in Fig. 9a, b and c as a function of applied magnetic field for the γFe_2O_3 particle, chemically stabilized and heat-stabilized albumin magnetic microspheres, respectively. Room temperature magnetization plots as a function of magnetic field show a small hysteresis loop. At 5 K, the hysteresis is rather sizable with a coercive field. The hysteresis loop is also symmetric about the center for both temperatures. This symmetric nature of the loop is a characteristic of superparamagnetic behavior [26]. The data on the magnetization–magnetic field plots at 5 K can be assumed to be below the blocking temperature of almost all the particles, whereas the data at 300 K suggest that there are still more particles which have not reached their blocking temperature, otherwise no hysteresis would be observed at that temperature, which is typical of the behavior of superparamagnetic particles [26]. In fact TEM micrographs of the maghemite particles show a wide distribution of particle sizes and the temperature–susceptibility (Fig. 8) also did not show any maxima, even at 300 K, indicating a wide range of blocking temperatures depending on the sizes of the particles.

Conclusion

Heat-stabilized microspheres are better dispersed than chemically cross-linked albumin microspheres. The particle size distribution analysis shows microspheres in the micron and submicron range. The submicron particles mostly have diameters between 0.3 to 0.8 μm. This certainly shows the probability of obtaining nanosized particles using the synthesis process described in this article. The optimization of the synthesis parameters needs additional studies. Backscattered electron imaging could be a very useful and information-providing tool for microspheres containing metals.

The surface structure of the microsphere was obtained in more detail by AFM than by SEM. TEM micrographs showed that maghemite particles used here are spherical in shape and have a wide size distribution.

The magnetic microspheres have a magnetic moment in an applied field but due to their wide size distribution and blocking temperature could not be obtained at or below room temperature. Superparamagnetic behavior was observed for the albumin magnetic microspheres synthesized.

References

1. Haik Y, Chen CJ, Pai V (1999) In: Shyy W (ed) Fluid dynamics on interfaces. Cambridge University Press, Cambridge, pp 439
2. Haik Y, Pai V, Chen CJ (1999) J Magn Magn Mater 194:254
3. Blanchard RJW, Grotenhuis I, Lafave JW, Perry JF Jr (1965) Proc Soc Exp Biol Med
4. Sugibayashi K, Morimoto Y, Nadai T, Kato Y (1977) Chem Pharm Bull 25:3433
5. Mary M (1997) In: Hafeli U, Schutt W, Zborowski M (eds) Scientific and clinical application of magnetic carriers. Plenum, New York, p 303
6. Assesnmacher M, Miltenyi S, Schmitz, J (1998) In: Hafeli U, Schutt W, Zborowski M (eds) Scientific and clinical application of magnetic carriers. Plenum, New York, p 68
7. Senyei AE, Widder KJ, Czerlinski G (1978) J Appl Phys 49:3578
8. Senyei AE, Widder KJ (1981) Gynol Oncol 12:1
9. Ishi F, Takamura A, Noro S (1984) Chem Pharm Bull 32:678
10. Wider KJ, Senyei AJ, Scarpelli DG (1978) Proc Soc Exp Biol Med 158:141
11. Iannotti JP, Baradet TC, Tobin M, Alavi A, Staum M (1991) J Orthop Res 9:432
12. Gupta PK, Hung CT, Perrier DG (1987) J Pharm Sci 76:141
13. Chatterjee J, Haik Y, Chen CJ (2001) J Magn Magn Mater 225:21
14. Gupta PK, Hung CT, Perrier DG (1986b) Int J Pharm 33:137
15. Gupta PK, Hung CT (1989) J Microencapsulation 6:427
16. Kojima T, Nakano M, Juni K, Inoue S, Yoshida Y (1984) Chem Pharm Bull 32: 2795
17. Lin JN, Drake B, Lea AS, Hansma PK, Andrade JD (1990) Langmuir 6:241
18. Kowalczyk D, Marsault JP, Slomkowski S (1996) Colloid Polym Sci 274:513
19. Hansma HG, Sinsheimen RL, Li MQ, Hansma PK (1992) Nucleic Acids Res 20:3585
20. Kraeft SK, Hafeli U, Chen LB (1997) In: Hafeli U, Schutt W, Teller J, Zborowski M (eds) Scientific and clinical application of magnetic carriers. Plenum, New York, p 149
21. Bishop HE (1966) In: Castaing R, Deschamps P, Philbert J (eds) Optique des rayons X et microanalyses. Herman, Paris, p 153
22. Gupta PK, Gallo JM, Hung CT, Perrier DG (1987) Drug Dev Ind Pharm 13:1471
23. Krinsley DH, Pye K, Boggs S Jr, Tovey NK (eds) (1998) Backscattered scanning electron microscopy and image analysis of sediments and sedimentary rocks, p 7
24. Heinrich KFJ (1966) In: Castaing R, Deschamps P, Philbert J (eds) Optique des rayons X et microanalyses. Herman, Paris, p 159
25. Malkinski LM, Wang JQ, Dai JB, Tang (1999) J Appl Phys Lett 75:844
26. Vassiliou JK, Mehrotra V, Russell MW, Giannelis EP, McMichael RD, Shull RD, Ziolo RF (1993) J Appl Phys 73:5109